

The Inherent Law of the Unpredictability of Financial Asset Price Fluctuations: Multistability and Chaos*

GU Enguo

DOI: 10.1007/s11424-024-1198-4

Received: 16 June 2023 / Revised: 5 September 2023

©The Editorial Office of JSSC & Springer-Verlag GmbH Germany 2024

Abstract This paper aims at understanding the price dynamics generated by the interaction of traders relying on heterogeneous expectations in an asset pricing model. In the present work the authors analyze a financial market populated by five types of boundedly rational speculators—two types of fundamentalists, two types of chartists and trend followers which submit buying/selling orders according to different trading rules. The authors formulate a stock market model represented as a 2 dimensional piecewise linear discontinuous map. The proposed contribution to the existing financial literature is two aspects. First, the authors perform study of the model involving a 2 dimensional piecewise linear discontinuous map through a combination of qualitative and quantitative methods. The authors focus on the existence conditions of chaos and the multi-stability regions in parameter plane. Related border collision bifurcation curves and basins of multi-attractors are also given. The authors find that chaos or quasi-period exists only in the case of fixed point being a saddle (regular or flip) and that the coexistence of multiple attractors may exist when the fixed point is an attractor, but it is common for spiral and flip fixed points.

Keywords BCB curve, chaos, financial market, heterogeneous agents, multiple attractors, piecewise linear discontinuous map.

1 Introduction

Stock market dynamics are excessively volatile and frequently display serious bubbles and crashes. Models with interacting heterogeneous speculators have proven their ability in explaining complex asset price behaviour, either from a theoretical or empirical point of view (see e.g., [1–6] among others). Over the last decade, agent-based financial market models have improved the understanding of the functioning of financial markets (see, for instance, [3, 7–9] and references therein). Modelling financial markets with heterogeneous agents demonstrated that


GU Enguo

Huanghe University of Science and Technology, Zhengzhou 450006, China.

Email: guenguo@hkhjxy193.wecom.work.

*This research was supported by the Fundamental Research Funds for the Central Universities, South-Central University for Nationalities under Grant No. CZT20006.

◊ *This paper was recommended for publication by Editor WANG Jue.*

 Springer

endogenous interactions between technical trading rules and fundamental trading rules may give rise to realistic asset price dynamics. A key feature is that heterogeneous interacting traders in financial markets are endowed by several behavioral rules, trade in the market. Heterogeneity and bounded rationality introduce non-linearity in the model which is a further element explaining complicated dynamics of prices in the market. A huge amount of deterministic and non-linear works in the heterogeneous agents framework have been proposed. For example, Naimzada AK^[10, 11] analyze a model with a switching mechanism and they show that complex dynamics can arise even if fundamentalist agents generate different fundamental values. [3, 12] show that technical traders can switch between several financial markets. Further, Agliari, et al.^[13] develop a stock market model in which participation depends upon an attractiveness measure related to the market activity and the fundamental value of the market. The authors show how the participation mechanism amplifies the occurrence of booms and busts dynamics. Others recent works of deterministic models with heterogeneous agents are, for example, those of [14–16].

The model established in this study is a piecewise linear discontinuous mapping model which is a nonlinear model. The main goal of our research is to explore the inherent laws of volatility and unpredictability in the financial system. As we all know, the chaos of the financial system is the main reason for the unpredictability of the internal law of price fluctuations in financial products. Therefore, exploring the chaos of the financial system helps to uncover the internal law of financial market fluctuations. Many dynamic models have been introduced to study the chaotic and hyperchaotic behavior of these systems^[17–19]. Multiple stability results in the simultaneous generation of multiple stable orbits. In fact, when several coexisting attractors are present in the system, the related basins may be not simple, and may be intermingled in a chaotic way, so that also a very small perturbation in the parameters of the systems may lead to a change of ω limit set of the trajectories.

Since Day and Huang propose bull and bear market models to explain the complex dynamics of financial markets, many scholars have studied the interaction of different rational traders who rely on simple trading rules to produce complex internal price changes^[2, 3, 20–23]. Tramontana, et al. have established and studied a one-dimensional discrete dynamic model containing two linear subsystems with two different types of traders: fundamentalists and chartists^[24–27]. According to whether these two types of traders are cautious in entering the market, they can be divided into direct market entry fundamentalists and cautious market entry fundamentalists, direct market entry chartists and cautious market entry chartists. On this basis, they have established and studied the 1-dimensional (1D) discrete dynamic model containing 3 linear subsystems. We take into account the inefficiency of the financial market, especially China's financial market, that is, due to factors such as information asymmetry, herd mentality, panic mentality, and other factors, investment strategies are often blind to a certain degree, and they will be subject to other peoples decisions. Influencing and imitating the investment behavior of others, results in the phenomenon of following suit in the investment market, and this irrational behavior is herding behavior. Herding behavior is closely related to the occurrence of financial crises and has a great impact on market stability. Some scholars believe that stylized laws such

as the distribution of fat tails in financial markets are related to the herd effect^[28]. This article considers that there are many follow-up speculators in China's financial market, abandoning the hypothesis of effective financial markets, assuming that there is another type of trend-following trader, they buy and sell according to recent price movements in the stock market, if the price of the market stock rises and accelerates, it will buy; if the price drops, it will be sold. As it turns out, the dynamics of our model is driven by a 2D piecewise linear discontinuous (PWLD) map with three branches.

As we all know, the dynamic system defined by the piecewise smooth function will have phenomena that the smooth system cannot, such as border collision bifurcation (BCB), slip and chattering. The most typical feature is BCB, which is a bifurcation that occurs when a point of a cycle collides with the boundary separating the different defined areas of the system. The BCB theory of piecewise smooth (PWS) continuous map has been developed and has been successfully applied to explain non-smooth bifurcation phenomena in physical systems. Since the 1990s, since many physical, engineering, economics and social systems have been described as non-smooth switching systems, a lot of research work has been directed to non-smooth switching systems. Such systems are usually given by two or more sets of differential equations, and the system is transferred from one set to another. In particular, several systems are modeled via discontinuous maps, often with several discontinuity points^[5, 29, 30]. Piecewise linear (PWL) map is usually a local approximation of a PWS map near the boundary. The bifurcation theory of 1D PWLD map with 2 subsystems has been well developed^[31–35]. However, the bifurcation theory of 1D piecewise linear discontinuous (PWLD) map with 3 subsystems is underdeveloped^[5, 26, 36, 37]. To the best of my knowledge, the bifurcation theory of 2D PWLD map with 3 different subsystems have not yet been investigated. The model established in this paper is described by a 2D PWLD map containing three linear asymmetrical subsystems. We have investigated 2D PWLD map with 3 subsystems but two outer subsystem are identical. The existence and stability conditions of periodic attractors and other bounded attractors are derived^[38]. We have established a calculation method for the BCB curves of 2D PWLD map with 2 subsystems and based on the BCB curves, we have determined the existence conditions of periodic orbit and the parameter range of the coexistence attractors^[39], as well as the related basins of multi-attractors in the phase space are described.

After this Introduction, the paper is structured as follows. In Section 2 we formulate a 2-dimensional discontinuous financial model. In Section 3, we describe some preliminary properties of its underlying dynamical system. Section 4 concerns periodic points and their classification. Section 5 includes the main part of our work, related to the new results, and it is structured in several subsections according five types of the fixed points. The existence conditions of chaos and cycles are derived. Multi-stability regions are described in the plane (m_L, m_R) by calculating relevant BCB curves. The basin of multiple attractors are presented in the phase space. Some discussions are given in Section 6. Section 7 concludes the paper.

2 The Dynamic Model

We assume a market maker mediates transactions out of equilibrium by providing or absorbing liquidity, depending on whether the excess demand is positive or negative. In addition to clearing the market, the market adjusts prices according to the following rule:

$$P_{t+1} = P_t + \mu(D_t^{C,1} + D_t^{F,1} + D_t^{C,2} + D_t^{F,2} + D_t^S), \tag{2.1}$$

where P is the log price, μ is a positive price adjustment parameter, and $D_t^{C,1}, D_t^{F,1}, D_t^{C,2}, D_t^{F,2}, D_t^S$ are the orders of the five types' speculators. Accordingly, excess buying drives the price up and excess selling drives it down. For simplicity, yet without loss of generality, we set scaling parameter μ equal to 1. Chartists believe in the persistence of bull and bear markets. The orders of type 1 chartists are therefore given by

$$D_t^{1,C} = \begin{cases} c^{1,a} + c^{1,b}(P_t - F), & P_t - F \geq 0, \\ -c^{1,c} + c^{1,d}(P_t - F), & P_t - F < 0, \end{cases} \tag{2.2}$$

where the reaction parameters $c^{1,a}, c^{1,b}, c^{1,c}, c^{1,d}$ are non-negative. Given their beliefs about future price movements, chartists of type 1 optimistically buy (pessimistically sell) if prices are in the bull (bear) market, that is, if the log price P is above (below) its log fundamental value F . As usual, the fundamental value is constant and known to all institutional investors and market participants. The reaction parameters $c^{1,a}$ and $c^{1,c}$ capture some general kind of optimism and pessimism, respectively, whereas the reaction parameters $c^{1,b}$ and $c^{1,d}$ indicate how aggressively chartists of type 1 trade on their perceived price signals.

Fundamentalists of type 1 expect prices to return towards their fundamental values. We thus write the orders placed by fundamentalists as

$$D_t^{1,F} = \begin{cases} -f^{1,a} + f^{1,b}(F - P_t), & P_t - F \geq 0, \\ f^{1,c} + f^{1,d}(F - P_t), & P_t - F < 0, \end{cases} \tag{2.3}$$

where again, the reaction parameters $f^{1,a}, f^{1,b}, f^{1,c}, f^{1,d}$ are non-negative. Hence fundamentalists of type 1 always trade in the opposite direction as chartists of type 1. In an overvalued market, they sell and in an undervalued market they buy. Similar to chartists of type 1, the trading intensity of fundamentalists of type 1 may depend on market circumstances: A certain mispricing in the bull market may trigger a higher or lower transaction than the same mispricing in the bear market. What type 1 chartists and fundamentalists have in common is that they are almost always active. Once they perceive a mispricing, they start trading. Type 2 chartists and type 2 fundamentalists are different to them in the sense that they only become active when the misalignment exceeds a certain critical threshold level. We assume in our model type 2 traders prefer to pay attention to market entry and to trade a fixed amount of assets. Type 2 chartists and fundamentalists submit orders according to

$$D_t^{C,2} = \begin{cases} c^{2,a}, & P_t - F \geq z, \\ 0, & |P_t - F| < z, \\ -c^{2,b}, & P_t - F \leq -z \end{cases} \tag{2.4}$$

and

$$D_t^{F,2} = \begin{cases} -f^{2,a}, & P_t - F \geq z, \\ 0, & |P_t - F| < z, \\ f^{2,b}, & P_t - F \leq -z, \end{cases} \quad (2.5)$$

respectively. The order sizes in the bull market are given by $c^{2,a} > 0$ and $f^{2,a} > 0$ while in the bear market they are given by $c^{2,b} > 0$ and $f^{2,b} > 0$ by type 2 chartists and fundamentalists, respectively, and the aforementioned threshold level is given by $z > 0$.

Trend-followers follow the trend blindly, and they place their orders based on a trend-extrapolation of past prices. Orders triggered by trend-followers may be written as

$$D_t^S = s^a + s^b(P_t - P_{t-1}), \quad (2.6)$$

where the parameters s^b is also non-negative to show trading aggressiveness of trend-followers, and s^a can be positive and negative to capture some general kind of optimism and pessimism. Insert (2.2)–(2.6) into (2.1) yields

$$P_{t+1} = P_t + s^a + s^b(P_t - P_{t-1}) + \begin{cases} m^1 + m^3 + s_1(P_t - F), & P_t - F \geq z, \\ m^1 + s_1(P_t - F), & 0 \leq P_t - F < z, \\ m^2 + s_2(P_t - F), & -z < P_t - F < 0, \\ m^2 + m^4 + s_2(P_t - F), & P_t - F \leq -z, \end{cases} \quad (2.7)$$

where $s_1 = c^{1,b} - f^{1,b}$, $s_2 = c^{1,d} - f^{1,d}$, $m^1 = c^{1,a} - f^{1,a}$, $m^2 = f^{1,c} - c^{1,c}$, $m^3 = c^{2,a} - f^{2,a}$, $m^4 = f^{2,b} - c^{2,b}$. Note first that s_1 , s_2 , m^1 , m^2 , m^3 and m^4 can take any values. Positive (negative) values of s_1 and s_2 mean that type 1 chartists are more (less) aggressive than type 1 fundamentalists in bull and bear markets, respectively. Of course, the same interpretation holds for m^3 and m^4 of type 2 speculators: A positive (negative) value of m^3 now means that type 2 chartists are more (less) aggressive than type 2 fundamentalists in bull markets, a positive (negative) value of m^4 now means that type 2 chartists are less (more) aggressive than type 2 fundamentalists in bear markets. m^1 and m^2 represent traders' expected difference of type 1 in bull and bear markets, respectively.

Introducing $u_t = P_t - F$ in (2.7), we obtain the following dynamical system

$$u_{t+1} = \begin{cases} (1 + s^b + s_1)u_t - s^b u_{t-1} + s^a + m^1 + m^3, & u_t \geq z, \\ (1 + s^b + s_1)u_t - s^b u_{t-1} + s^a + m^1, & 0 \leq u_t < z, \\ (1 + s^b + s_2)u_t - s^b u_{t-1} + s^a + m^2, & -z < u_t < 0, \\ (1 + s^b + s_2)u_t - s^b u_{t-1} + s^a + m^2 + m^4, & u_t \leq -z. \end{cases} \quad (2.8)$$

Let us write $v_t = -s^b u_{t-1}$ and consider the case that the difference in aggressiveness and expectations between type 1 traders is the same in a bull market and a bear market. That is, let $s^1 = s^2 \triangleq s$, $m^1 = m^2 \triangleq \bar{m}$, then (2.8) can be expressed as two dimensional discontinuous

map

$$T : \begin{pmatrix} u \\ v \end{pmatrix}' = \begin{cases} A_R \begin{pmatrix} u \\ v \end{pmatrix} + (\alpha + m^3)e_1, & u \geq z, \\ A_M \begin{pmatrix} u \\ v \end{pmatrix} + \alpha e_1, & |u| < z, \\ A_L \begin{pmatrix} u \\ v \end{pmatrix} + (\alpha + m^4)e_1, & u \leq -z, \end{cases} \tag{2.9}$$

where ' denotes the unit-time advancement operator,

$$\alpha = s^a + \overline{m}, \quad A_L = A_M = A_R \triangleq A = \begin{pmatrix} 1 + s^b + s & 1 \\ -s^b & 0 \end{pmatrix}.$$

The map T has three branches, one locates in the middle region enclosed by two borders $x = -1$ and $x = 1$ (denoted by T_M), the others locate outer of the region. One is in the left side of the range $|x| < 1$ (denoted by T_L), the other in the right side of the range $|x| < 1$ (denoted by T_R). This is the map that we shall explore in detail in the rest of the paper. In this paper, we analyze the map under the following assumption:

Assumption The condition $0 < s^b < 1$ is assumed hereafter. All the results that follow rely on this assumption.

3 Some Preliminary Properties

The first property is that parameter z is a scale variable.

Theorem 3.1 *The map T in (2.9) is topologically conjugated to the map in (3.1).*

Proof In fact, by using the change of variable $x = u/z, y = v/z$ and defining the aggregate parameter $m = \alpha/z, m_L = (\alpha + m^4)/z, m_R = (\alpha + m^3)/z$, our model in (2.9) becomes

$$T : X' = \begin{cases} T_L(X) = AX + m_L e_1, & x \leq -1, \\ T_M(X) = AX + m e_1, & -1 < x < 1, \\ T_R(X) = AX + m_R e_1, & x \geq 1, \end{cases} \tag{3.1}$$

where $X = \begin{pmatrix} x \\ y \end{pmatrix}$, and T is represented by a 2D PWLD map with two discontinuity borders. ■

Note that parameters

$$\begin{aligned} m_L &= \frac{s^a + c^{1,a} - f^{1,a} + c^{2,a} - f^{2,a}}{z}, \\ m &= \frac{s^a + c^{1,a} - f^{1,a}}{z}, \\ m_R &= \frac{s^a + c^{1,a} - f^{1,a} + f^{2,b} - c^{2,b}}{z} \end{aligned}$$

are aggregation parameters and they can be positive, negative or zero. $s = c^{1,b} - f^{1,b} = c^{1,d} - f^{1,d}$ can also be positive, negative or zero. If $s > 0$, chartists of type 1 dominate fundamentalists of type 1 in bull and bear markets and vice versa. s^b is always positive. If $s^b \geq 1$ which is contrary to above assumption, for example, $s^b = 1$, the map (3.1) is area-preserving mapping (conservative system). It has very complex dynamic behavior. We shall leave this discussion for the future.

Now, we shall show that the two cases with a positive and negative sign of m_L, m, m_R are topologically conjugated to one another. Denoting T by $T(x, y; s^b, s, m_L, m, m_R)$, we have the following

Theorem 3.2 *The map T in (3.1) with $m_L > 0, m > 0, m_R > 0$ is topologically conjugated with the same map with $m_L < 0, m < 0, m_R < 0$, and $T(-x, -y; s^b, s, -m_L, -m, -m_R) = -T(x, y; s^b, s, m_L, m, m_R)$.*

Proof In fact, by using the change of variable $x = -u, y = -v$, the map in (3.1) leads to

$$T : \begin{pmatrix} u \\ v \end{pmatrix}' = \begin{cases} A \begin{pmatrix} u \\ v \end{pmatrix} - m_L e_1, & u \geq 1, \\ A \begin{pmatrix} u \\ v \end{pmatrix} - m e_1, & |u| < 1, \\ A \begin{pmatrix} u \\ v \end{pmatrix} - m_R e_1, & u \leq -1. \end{cases} \quad (3.2)$$

The proof is finished. ■

This property means that when given s^b and s , conclusions for (m_L, m, m_R) also hold for $(-m_L, -m, -m_R)$. As $x < -1$ (or $x > 1$), $-x > 1$ (or $-x < -1$) and the middle region does not change during the transformation, results of only involving middle side and left side for (m, m_L) also hold for results of only involving middle side and right side for $(-m, -m_R)$.

Theorem 3.3 *The map T in (3.1) is a invertible map all over its domain except $x = \pm 1$.*

Proof In fact, from (3.1) we have

$$T^{-1} : \begin{cases} T_B^{-1}(X) = B_B X - m_R e_2, & y' \leq -s^b, \\ T_M^{-1}(X) = B_M X - m e_2, & -s^b < y' < s^b, \\ T_A^{-1}(X) = B_A X - m_L e_2, & y' \geq s^b, \end{cases} \quad (3.3)$$

where

$$B_A = B_B = B_M = \begin{pmatrix} 0 & -\frac{1}{s^b} \\ 1 & \frac{1+s^b+s}{s^b} \end{pmatrix}$$

and $e_2 = \begin{pmatrix} 0 \\ 1 \end{pmatrix}$. The map T^{-1} has three branches, one locates in the middle region enclosed by two borders $y' = -s^b$ and $y' = s^b$ (denoted by T_M^{-1}), the others locate outer of the region. One

is above the range $|y'| < s^b$ (denoted by T_A^{-1}), the other below the range $|y'| < s^b$ (denoted by T_B^{-1}). To prove the map (3.1) is invertible all over its domain, we rewrite the map (3.1) over its domain except $x = \pm 1$ as

$$T : X' = \begin{cases} T_L(X) : (-\infty, -1) \times R \rightarrow \Omega_1, \\ T_M(X) : (-1, 1) \times R \rightarrow \Omega_2, \\ T_R(X) : (1, +\infty) \times R \rightarrow \Omega_3. \end{cases}$$

Because $y' = -s^b x$ and $s^b > 0$, so

$$\Omega_1 = R \times (s^b, +\infty), \quad \Omega_2 = R \times (-s^b, +s^b), \quad \Omega_3 = R \times (-\infty, -s^b).$$

Therefore, we have $\Omega_1 \cap \Omega_2 \cap \Omega_3 = \emptyset$. The map T in (3.1) is a invertible map all over its domain except $x = \pm 1$. ■

4 Periodic Points and Their Classification

The fixed points of the system (3.1) (also called as 1-cycle) in three regions of the domain are given by

$$\begin{aligned} L^* &= \left(-\frac{m_L}{s}, \frac{s^b m_L}{s} \right), \\ M^* &= \left(-\frac{m}{s}, \frac{s^b m}{s} \right), \\ R^* &= \left(-\frac{m_R}{s}, \frac{s^b m_R}{s} \right). \end{aligned} \tag{4.1}$$

According to the existence of fixed points, we can divide them into two categories: Real and virtual fixed points. If the fixed points locate their suitable regions, they exists and are called real fixed points, otherwise it does not. However, when they do not exist, dynamic behaviour is influenced by the “nonexistent” fixed points, which are called “virtual” fixed points, and are denoted by $\bar{L}^*, \bar{M}^*, \bar{R}^*$, respectively. According to the characteristics of eigenvalues of A , we can classify them into five types. The fixed points are stable when their eigenvalues are less than 1 in magnitude. This is true only when A satisfies the three Jury conditions:

$$\begin{aligned} P1 &= 1 - \text{Tr}A + \text{Det}A = -s > 0, \\ P2 &= 1 + \text{Tr}(A) + \text{Det}A = s + 2(1 + s^b) > 0, \\ P3 &= 1 - \text{Det}A = 1 - s^b > 0. \end{aligned}$$

Characteristic equation of A is $\lambda^2 - (1 + s^b + s)\lambda + s^b = 0$. If $\Delta = (1 + s^b + s)^2 - 4s^b = (1 - s^b)^2 + 2(1 + s^b)s + s^2 < 0$, matrix A will have a pair of conjugate complex eigenvalues, that is, all fixed points are spiral attractors as the parameters satisfy the three Jury conditions and $-(1 + s^b) - 2\sqrt{s^b} < s < -(1 + s^b) + 2\sqrt{s^b}$. As we have set $0 < s^b < 1$, thus, for such a map, there are five basic types of fixed points as shown in Figure 1.

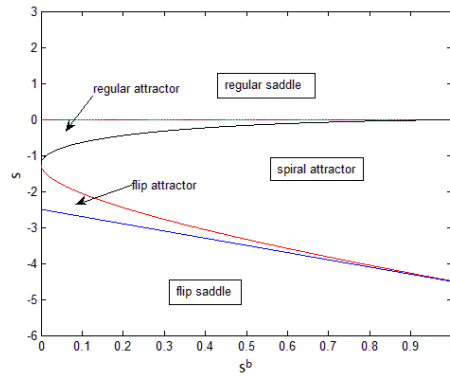


Figure 1 Five basic types of fixed points in the parameter space (s^b, s)

Let us now analyze the conditions leading to higher periodic dynamics. Let $\mathcal{S} : \mathbb{Z} \rightarrow \{L, M, R\}$ be a periodic symbol sequence with minimal period $n, n \geq 1$ (that is, $\mathcal{S}_{i+n} = \mathcal{S}_i$ for all $n \geq 1$). For a periodic symbol sequence $\mathcal{S}_0, \mathcal{S}_1, \dots, \mathcal{S}_{n-1}$, let $T^{\mathcal{S}} = T^{\mathcal{S}_{n-1}} \circ \dots \circ T^{\mathcal{S}_1} \circ T^{\mathcal{S}_0}$ denote the iteration of T following \mathcal{S} . A straightforward expansion leads to

$$T^{\mathcal{S}}X = A^n X + P_{\mathcal{S}}e_1, \tag{4.2}$$

where

$$P_{\mathcal{S}} = m^{\mathcal{S}_{n-1}}I + m^{\mathcal{S}_{n-2}}A + \dots + m^{\mathcal{S}_0}A^{n-1}.$$

Let $\mathcal{S}^{(i)}$ denote the i th shift permutation of \mathcal{S} (e.g., if $\mathcal{S} = LLMR$, then $\mathcal{S}^{(2)} = MRLL$). The i th point of an \mathcal{S} -cycle, denoted by $X_i^{\mathcal{S}} = (x_i^{\mathcal{S}}, y_i^{\mathcal{S}})$, is a fixed point of $T^{\mathcal{S}^{(i)}}$. When $I - A^n$ is nonsingular, this point is unique. If $\det(I - A^n) \neq 0$ then for each i

$$X_i^{\mathcal{S}} = (I - A^n)^{-1}P_{\mathcal{S}^{(i)}}e_1. \tag{4.3}$$

An \mathcal{S} -period is real if every point

$$x_i^{\mathcal{S}} = \frac{e_1^T \text{adj}(I - A^n) P_{\mathcal{S}^{(i)}} e_1}{\det(I - A^n)} \tag{4.4}$$

lies on the “correct” region. If one of points $x_i^{\mathcal{S}}$ lies on the “wrong” region, an \mathcal{S} -period is virtual. For example, if X is a periodic point of an n -cycle with symbolic sequence $\mathcal{S} = L^p M^q R^r$, where p is the number of periodic points of the n -cycle in the region $x < -1$ and q in the region $|x| < 1$ and r in the region $x > 1$, with $p + q + r = n$ and at least two of parameters p, q, r are not equal to 0, then $P_{\mathcal{S}} = I + m_R(A + \dots + A^{r-1}) + m(A^r + \dots + A^{r+q-1}) + m_L(A^{n-p+1} + \dots + A^{n-1})$, we have

$$X = (I - A^n)^{-1}P_{\mathcal{S}}e_1.$$

X is stable if and only if all eigenvalues of A^n lies in the unit circle. Simple calculations we find that if the eigenvalues of A are λ_1, λ_2 , the eigenvalues of A^n are λ_1^n, λ_2^n . Similar to the fixed point, according to the characteristics of eigenvalues of A^n , we can divide n -cycle into 5 types. We have the following:

Theorem 4.1 1) If $s > 0$, n -cycle is a regular saddle;

2) If $-(1+s) + 2\sqrt{s^b} < s < 0$, n -cycle is a regular attractor;

3) If $-(1+s) - 2\sqrt{s^b} < s < -(1+s) + 2\sqrt{s^b}$, n -cycle is a spiral attractor;

4) If $-2s^b - 2 < s < -(1+s) - 2\sqrt{s^b}$, $2k$ -cycle is a regular attractor and $2k+1$ -cycle is a flip attractor;

5) If $s < -2s^b - 2$, $2k$ -cycle is a regular saddle and $2k+1$ -cycle is a flip saddle.

Proof 1) If $s > 0$, the eigenvalues of A satisfy $\lambda_1 > 1 > \lambda_2 > 0$. The eigenvalues of A^n satisfy $\lambda_1^n > 1 > \lambda_2^n > 0$, so n -cycle is a regular saddle.

2) If $-(1+s) + 2\sqrt{s^b} < s < 0$, the eigenvalues of A satisfy $1 > \lambda_1, \lambda_2 > 0$. The eigenvalues of A^n satisfy $1 > \lambda_1^n, \lambda_2^n > 0$, so n -cycle is a regular attractor.

3) If $-(1+s) - 2\sqrt{s^b} < s < -(1+s) + 2\sqrt{s^b}$, the eigenvalues of A satisfy $|\lambda_1| < 1, |\lambda_2| < 1$. The eigenvalues of A^n satisfy $|\lambda_1^n| < 1, |\lambda_2^n| < 1$, so n -cycle is a spiral attractor.

4) If $-2s^b - 2 < s < -(1+s) - 2\sqrt{s^b}$, the eigenvalues of A satisfy $-1 < \lambda_1, \lambda_2 < 0$. If $n = 2k$, the eigenvalues of A^n satisfy $1 > \lambda_1^n, \lambda_2^n > 0$, so $2k$ -cycle is a regular attractor. If $n = 2k+1$, the eigenvalues of A^n satisfy $-1 < \lambda_1^n, \lambda_2^n < 0$, so $2k+1$ -cycle is a flip attractor.

5) If $s < -2s^b - 2$, the eigenvalues of A satisfy $\lambda_1 < -1 < \lambda_2 < 0$. If $n = 2k$, the eigenvalues of A^n satisfy $\lambda_1^n > 1 > \lambda_2^n > 0$, so $2k$ -cycle is a regular saddle. If $n = 2k+1$, the eigenvalues of A^n satisfy $\lambda_1^n < -1 < \lambda_2^n < 0$, so $2k+1$ -cycle is a flip saddle. \blacksquare

If $-2s^b - 2 < s < 0$, any cycle of map T in (3.1) is an attractor, that is, map T has no saddle periodic point, and thus no chaotic attractors. If $s > 0$ or $s < -2s^b - 2$, any cycle of map T is a saddle, that is, map T has no periodic attractor, and thus may have chaotic attractors. n -cycle has the same type as fixed point when it is a regular saddle, regular attractor, spiral attractor. However, when fixed point is flip attractor or saddle, for the same matrix A , odd n -cycles have the same type as fixed points and even n -cycle becomes a regular attractor or saddle.

5 Dynamics of Model with Different Types of Fixed Point

In this section, we classify the dynamics of the discontinuous system (3.1) depending on the different types of fixed points. We shall study the effect of the position of the fixed points on the dynamics of the system (3.1) for given parameters s^b, s . Noting the expressions of fixed points (4.1), for fixed parameters s^b, s which determine the stability types of fixed points, the position of the fixed points depend on the parameters m_L, m and m_R . In fact, we shall study the dynamics of the system with the different types of fixed points as the parameters m_L, m and m_R are varied.

5.1 Regular Saddle Fixed Points $s > 0$

As $s > 0$ and noting $0 < s^b < 1$, all fixed points are regular saddle whether they exist (real or virtual). In this case, the eigenvalues of A satisfy $0 < \lambda_2 < 1 < \lambda_1$. Dynamic behavior of the system (3.1) can be roughly seen through the 2-dimensional bifurcation diagram of Figure 2 obtained with $s^b = 0.8, s = 0.1, m = 0.2$. Figure 2 shows the system (3.1) either divergent or tends to a periodic attractor with a period exceeding 10. From Theorem 4.1 we know that the

system (3.1) has no periodic attractor, all bounded attractors are chaos or quasi-period.

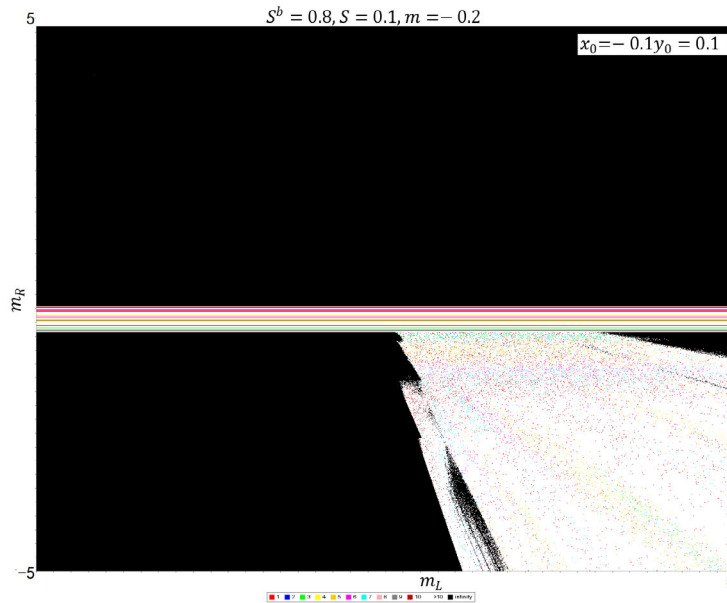


Figure 2 The 2-dimensional bifurcation diagram in parameter plane (m_L, m_R) obtained with $s^b = 0.8, s = 0.1, m = 0.2$

About the divergence of the system (3.1), we have the following:

Theorem 5.1 (*Divergence*) Suppose $s > 0$, consider the map T .

- 1) If $m_L < s$ and $m_R > -s$, then any initial condition other than M^* leads to a divergent trajectory;
- 2) If $m > s$ and $m_R > -s$, then any initial condition other than L^* leads to a divergent trajectory;
- 3) If $m < -s$ and $m_L < s$, then any initial condition other than R^* leads to a divergent trajectory.

Proof 1) As $s > 0$, the fixed point M^* is regular saddle whether it is real or virtual, trajectory starting from any initial condition in the middle region $|x| < 1$ other than M^* (when it is real) will go out of the region along the unstable manifolds of M^* . Noting $m_L < s$ and $m_R > -s$, both \bar{L}^* and \bar{R}^* are virtual regular saddle. Trajectories from the points in the outer region $|x| > 1$ tends to infinity along the unstable manifolds of \bar{L}^* or \bar{R}^* , which also exist in the region $|x| > 1$.

2) If $m_L < s$, noting $m_R > -s$, 2) holds from conclusion in 1); If $m_L > s$, L^* is real regular saddle. Except that the stable manifold of L^* is parallel to the x axis, trajectories from any point in the left region $x < -1$ and in the left side of stable manifold of L^* tends to infinity along the unstable manifold of L^* , while the trajectory from any point in the right side of stable manifold of L^* enters the middle region along the unstable manifolds of L^* . Noting $m > s$, \bar{M}^* locates in the left region. Trajectory starting from any initial condition in the middle region $|x| < 1$ goes into the right region along the unstable manifolds of \bar{M}^* , which also exist in the

region $|x| < 1$. Similarly, trajectory from any point in the right region $x > 1$ tends to infinity along the unstable manifolds of \overline{R}^* , which also exist in the region $x > 1$.

3) As 2) holds for any m_L , that is, the system (3.1) having a divergent trajectory only involves the conditions $m > s$ and $m_R > -s$, from Theorem 3.2, the conclusion of 2) still holds after replacing m and m_R with $-m$ and $-m_L$. Therefore, 3) holds due to symmetry. \blacksquare

From Theorem 4.1, about the attractor of the system (3.1), we have the following:

Theorem 5.2 (*Local chaotic or quasi-periodic attractors*) Suppose $s > 0$, consider the map T with one of the following conditions:

1) $m_L > s$, $|m| < s$ and $m_R < -s$;

2) $m > s$ and $\exists c_2 > c_1 > 1$ such that $-c_2s < m_R < -c_1s$ or $m < -s$ and $\exists c_2 > c_1 > 1$ such that $c_2s > m_L > c_1s$;

3) $m_L > s$, $|m| < s$ and $m_R > -s$ or $m_R < -s$, $|m| < s$ and $m_L < s$;

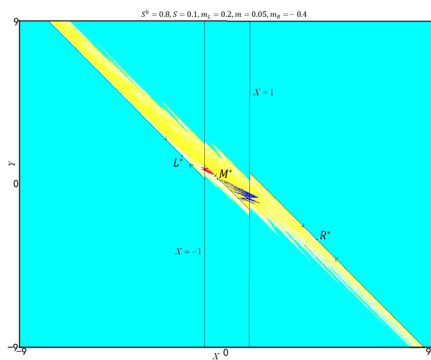
then trajectory from the point of attraction basin in the plane converges to chaotic or quasi-periodic attractors (chaotic attractors in most cases).

Proof 1) As $s > 0$, if $m_L > s$, $|m| < s$ and $m_R < -s$, all fixed points L^*, M^*, R^* are real regular saddle. As the stable manifolds of the saddle fixed points L^*, M^*, R^* are invariant set. Except that the stable manifold of L^* denoted by $W_{L^*}^s$ is parallel to x axis, trajectory starting from any point in left side of $W_{L^*}^s$ tends to infinity along the unstable manifold of L^* and in the right side of $W_{L^*}^s$ goes to the middle region along the unstable manifold of L^* . Similarly, except that the stable manifold $W_{M^*}^s$ is parallel to x axis, trajectory starting from any point in the right side of $W_{M^*}^s$ goes to the right region along the unstable manifold of M^* and in left side of $W_{M^*}^s$ goes to the left region along the unstable manifold of M^* and then goes back due to the unstable manifold of L^* . This forms a bounded attractor between $W_{L^*}^s$ and $W_{M^*}^s$. From Theorem 4.1, this bounded attractor can not be a periodic attractor, it may be a chaotic or quasi-periodic attractor. Symmetrically, another bounded attractor between $W_{R^*}^s$ and $W_{M^*}^s$ may be formed due to interaction between the unstable manifolds of M^* and R^* . The basin of these two bounded attractors is bounded by the preimages of $W_{L^*}^s$ and $W_{R^*}^s$ and the preimages of borders $x = \pm 1$, and the boundaries separating coexistence bounded attractors are the preimages of stable manifold $W_{M^*}^s$ (see Figure 3(a)).

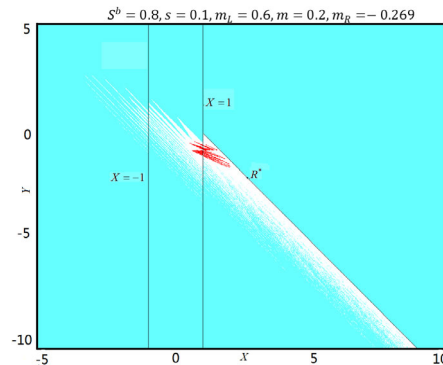
2) If $m > s$ and $\exists c_2 > c_1 > 1$ such that $-c_2s < m_R < -c_1s < -s$, virtual regular saddle \overline{M}^* locates in the left region and real regular saddle R^* is a suitable distance away from the discontinuous border on the right. Whether L^* exists or not, trajectories from some points in the left region may enter the middle region along the unstable manifolds of \overline{M}^* and trajectories from some points may tend to infinity along the unstable manifolds of \overline{M}^* . Trajectories from some points in the middle regions go into the right region along the unstable manifolds of \overline{M}^* , which also exist in the region $|x| < 1$. Except that the stable manifold of R^* denoted by $W_{R^*}^s$ is parallel to x axis, trajectory starting from any point in right side of $W_{R^*}^s$ tends to infinity along the unstable manifold of R^* and in the left side of $W_{R^*}^s$ goes to the middle region along the unstable manifold of R^* and then may come back due to the unstable manifolds of \overline{M}^* . This forms a bounded attractor between $W_{R^*}^s$ and $x = -1$, which is a chaotic or quasi-periodic

attractor. $W_{R^*}^s$ is a part of left boundary of basin (see Figure 3(b)). If $m < -s$ and $\exists c_2 > c_1 > 1$ such that $c_2 s > m_L > c_1 s > s$, from symmetry Theorem 3.2 we know that trajectory from the point of attraction basin in the plane converges to a chaotic or quasi-periodic attractor between $W_{L^*}^s$ and $x = 1$.

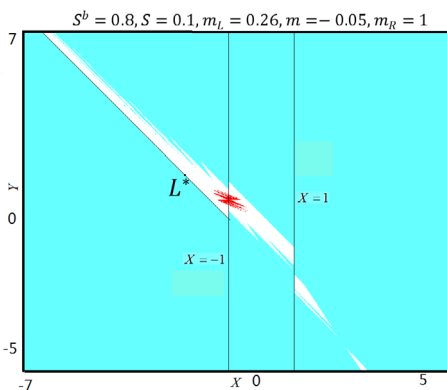
3) If $m_L > s$, $|m| < s$ and $m_R > -s$, L^* and M^* are real regular saddles and $\overline{R^*}$ is a virtual regular saddle. From the proof of 1), except that the stable manifold of L^* denoted by $W_{L^*}^s$ is parallel to x axis, there is a chaotic or quasi-periodic attractor between $W_{L^*}^s$ and $W_{M^*}^s$. The basin of the attractor is bounded by the preimages of $W_{L^*}^s$ and $W_{M^*}^s$ and the preimages of borders $x = \pm 1$ (see Figure 3(c)). Therefore, trajectory from the point of attraction basin in the plane converges to a chaotic or quasi-periodic attractor. If $m_R < -s$, $|m| < s$ and $m_L < s$, a chaotic or quasi-periodic attractor between $W_{R^*}^s$ and $W_{M^*}^s$ also exists due to symmetry Theorem 3.2. ■



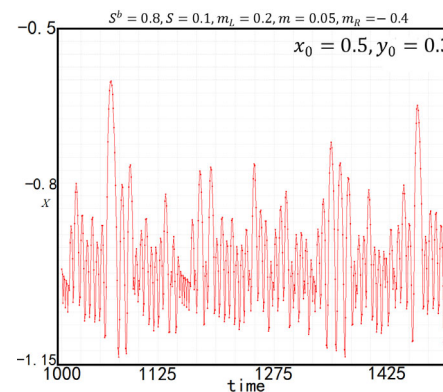
(a)



(b)



(c)



(d)

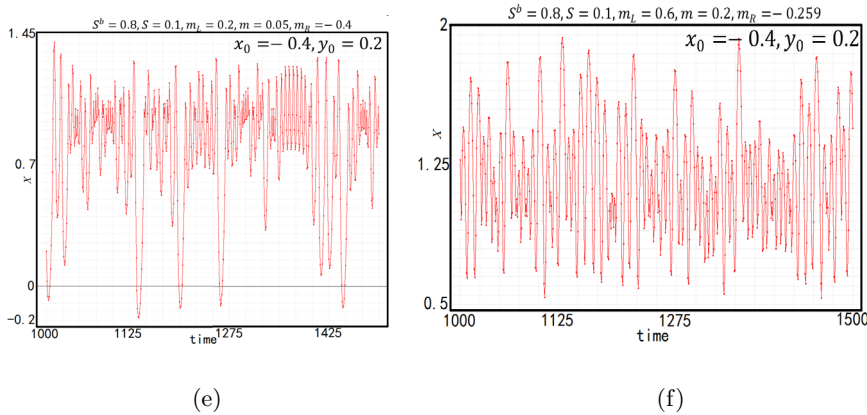


Figure 3 Basins of attractors in phase space, (a) coexistent chaotic attractors and their basins obtained with $s^b = 0.8, s = 0.1, m_L = 0.2, m = 0.05, m_R = -0.4$, (b) chaotic attractor between $W_{R^*}^s$ and $x = -1$ and its basin obtained with $s^b = 0.8, s = 0.1, m_L = 0.6, m = 0.2, m_R = -0.269$, (c) chaotic attractor between between $W_{L^*}^s$ and $W_{M^*}^s$ and its basin obtained with $s^b = 0.8, s = 0.1, m_L = 0.26, m = -0.05, m_R = 1$, (d) time series obtained with parameters $s^b = 0.8, s = 0.1, m_L = 0.2, m = 0.05, m_R = -0.4$ and initial value $x_0 = 0.5, y_0 = 0.3$, (e) time series obtained with parameters $s^b = 0.8, s = 0.1, m_L = 0.2, m = 0.05, m_R = -0.4$ and initial value $x_0 = -0.4, y_0 = 0.2$, (f) time series obtained with parameters $s^b = 0.8, s = 0.1, m_L = 0.6, m = 0.2, m_R = -0.259$ and initial value $x_0 = -0.4, y_0 = 0.2$

Note that $x = \frac{P-F}{z}, y = -s^b x$ are state variables. If $x > 0$, asset prices exceed fundamental values and we think that financial markets are in a bull market. If $x < 0$, asset prices exceed fundamental values and we think that financial markets are in a bear market. If the asset price fluctuates around $x = 0$, we think that financial markets are in a bear market. we think financial markets are in a bear/bull transition. The initial iteration value of Figure 3(d) was taken in the yellow region of Figure 3(a), thus converging to the blue one of the coexistence attractors of Figure 3(a), while the initial value of Figure 3(e) was taken in the white region of Figure 3(a), thus converging to the red one of the coexistence attractors of Figure 3(a). The initial iteration value of Figure 3(f) is taken in the white region of Figure 3(b), thus converging to the red attractor of Figure 3(b). As seen in Figure 3(d), time series of the system (3.1) is completely above $x = 0$ which means that the financial market is in a bear market with random fluctuations. As seen in Figure 3(e), time series of the system (3.1) spans $x = 0$, which means that the financial market is in a bear/bull transition with random fluctuations. As seen in Figure 3(f), time series of the system (3.1) is completely below $x = 0$ which means that the financial market is in a bull market with random fluctuations.

5.2 Regular Attracting Fixed Points $-(1 + s^b) + 2\sqrt{s^b} < s < 0$

Theorem 5.3 (Attracting fixed points) Suppose $-(1 + s^b) + 2\sqrt{s^b} < s < 0$, consider the map T .

- 1) If $|m| < -s$, $m_L > s$, and $m_R < -s$, then trajectory from any point in the plane converges to M^* , that is M^* is a globally attracting fixed point;
- 2) If $|m| < -s$, $m_L < s$, and $m_R < -s$, then attracting fixed points M^* and L^* coexist with their basins separated by preimages of the border lines $x = -1$;
- 3) If $|m| < -s$, $m_L > s$, and $m_R > -s$, then attracting fixed points M^* and R^* coexist with their basins separated by preimages of the border lines $x = 1$;
- 4) If $|m| < -s$, $m_L < s$, and $m_R > -s$, then three attracting fixed points M^* , L^* and R^* coexist with their basins separated by preimages of the border lines $x = \pm 1$;
- 5) If $m > -s$, $m_R > -s$, then trajectory from any point in the plane converges to R^* or coexistence attractors L^*, R^* ;
- 6) If $m < s$, $m_L < s$, then trajectory from any point in the plane converges to L^* or coexistence attractors L^*, R^* .

Proof 1) As $-(1+s^b)+2\sqrt{s^b} < s < 0$, if $|m| < -s$, $m_L > s$, and $m_R < -s$, fixed point M^* is a real regular attractor, \bar{L}^* and \bar{R}^* are virtual regular fixed points. If \bar{L}^* locates in the middle region, all the points in the left region are attracted to the middle region and then converge to M^* . If \bar{L}^* locates in the right region, all the points in the left region are attracted to the right region, but, trajectories from them must pass through the middle region before reaching the right region. When they reach the middle region they are attracted to M^* . Symmetrically, If \bar{R}^* locates in the middle region or the left region, all the points in the right region are attracted to the middle region and then converge to M^* . Trajectory from any point in middle region tend to fixed point M^* . Therefore, trajectory from any point of in the plane converges to M^* .

2) If $|m| < -s$, $m_L < s$, and $m_R < -s$, fixed point M^* and L^* are real attractors, \bar{R}^* is a virtual regular fixed point. Trajectory from any point in the middle region converges to M^* and in the left region to L^* . If \bar{R}^* locates in the middle region or the left region, all the points in the right region are attracted to the middle region or the left region and then converge to M^* or L^* , which are coexistence attractors. As the eigenvalues of A satisfy $0 < \lambda_1, \lambda_2 < 1$, the eigenvalues of A^n satisfy $0 < \lambda_1^n, \lambda_2^n < 1$. Therefore, any periodic point can not be a saddle in this case, the boundaries of basins of coexistence attractors are thus separated by preimages of the border lines $x = -1$.

3) If $|m| < -s$, $m_L > s$, and $m_R > -s$, fixed point M^* and R^* are real attractors, \bar{L}^* is a virtual regular fixed point. From the symmetry Theorem 3.2 and the conclusion of 2), then attracting fixed points M^* and R^* coexist with their basins separated by preimages of the border lines $x = 1$.

4) If $|m| < -s$, $m_L < s$, and $m_R > -s$, all fixed points are real attractors. As there is no saddle periodic point in this case (see Theorem 4.1), they coexist with their basins separated by preimages of the border lines $x = \pm 1$ (see Figure 4(a)).

5) If $m > -s$, $m_R > -s$ fixed point \bar{M}^* is a virtual regular attractor located in the right region, R^* is a real regular fixed point. Any point in the middle region is attracted to the right region and then converges to R^* . If $m_L > s$, \bar{L}^* is a virtual regular fixed point. Any point in the left region is attracted to the middle and then to right region and finally converges to R^* .

If $m_L < s$, noting $m_R > -s$, L^*, R^* are attracting fixed points and they attract the points in the left and right region, respectively. They coexist with their basins separated by preimages of the border lines $x = \pm 1$.

6) As 6) is the symmetry of 5), the conclusion of 6) holds by Theorem 3.2. \blacksquare

Theorem 5.4 (*Attracting cycles*) Suppose $-(1 + s^b) + 2\sqrt{s^b} < s < 0$, consider the map T .

1) If $m > -s$ and $|m_R| < -s$, the system (3.1) has a periodic attractor. If $m_L > s$, then trajectory from any point in the plane converges to the periodic attractor. If $m_L < s$ then the periodic attractor coexists with attracting fixed points L^* with their basins separated by preimages of the border lines $x = -1$;

2) If $m < s$ and $|m_L| < -s$, the system (3.1) has a periodic attractor. If $m_R < -s$, then trajectory from any point in the plane converges to the periodic attractor. If $m_R > -s$ then the periodic attractor coexists with attracting fixed points R^* with their basins separated by preimages of the border lines $x = 1$;

3) If $m > -s$ and $m_L < m_R < s$, then the system (3.1) may have a periodic attractor coexisting with L^* or globally converge to L^* .

4) If $m < s$ and $-s < m_L < m_R$, then the system (3.1) may have a periodic attractor coexisting with R^* or globally converge to R^* .

5) If $m > -s, m_L > s$ and $m_R < -s$, then the system (3.1) has a periodic attractor in the right side of $x = -1$.

6) If $m < s, m_R < -s$ and $m_L > s$, then the system (3.1) has a periodic attractor in the left side of $x = 1$.

Proof As the cases 2), 4) and 6) are the symmetry of 1), 3) and 5), respectively, we only gave the proof of 1), 3) and 5).

1) If $m > -s$ and $|m_R| < -s$, virtual regular fixed points \overline{M}^* and \overline{R}^* locate in the right and middle regions, respectively. Points in the middle region are attracted to the right region by \overline{M}^* and then are attracted to the middle region by \overline{R}^* and then come back due to the influence of \overline{M}^* . This forms a bounded attractor between \overline{M}^* and \overline{R}^* . From Theorem 5.4, it is impossible for the system (3.1) to have a periodic saddle, therefore, there is no homoclinic chaos, so the bounded attractor is a periodic attractor. If $m_L > s$, \overline{L}^* is a virtual regular fixed point, all the points in the left region are attracted to the middle or right regions and then converge to the periodic attractor. If $m_L < s$, L^* is also an attractor, then the periodic attractor coexists with attracting fixed points L^* with their basins separated by preimages of the border lines $x = -1$, since the system (3.1) has no periodic saddle in this case.

3) If $m > -s$ and $m_L < m_R < s$, fixed point \overline{M}^* locates in the right region, fixed point L^* is a real attractor, virtual regular fixed point \overline{R}^* locates between L^* and the left border $x = -1$. Trajectories from points in the right region are attracted to the left region by \overline{R}^* but they must pass through the middle region. As soon as they reach the middle region, some may be attracted back to the right region by \overline{M}^* , a periodic attractor is formed similar to 1). Some of them may be attracted to the left region by \overline{R}^* , and as they pass through the middle region,

they will converge to fixed point L^* . If all the points in the right region are attracted to the left region by \overline{R}^* , L^* is a globally attractor. If part of them pass through the middle region, a periodic attractor coexists with L^* (see Figure 4(b)).

5) If $m > -s, m_L > s$ and $m_R < -s$, all fixed points are virtual regular fixed points. If $s < m_R < -s$, the conclusion holds from the proof process of 1). If $m_R < s$, \overline{R}^* locates in the left region. Trajectories from points in the right region are attracted to the left region by \overline{R}^* , but they must pass through the middle region. As soon as they reach the middle region, they are attracted back to the right region by \overline{M}^* , this forms a periodic attractor. ▀

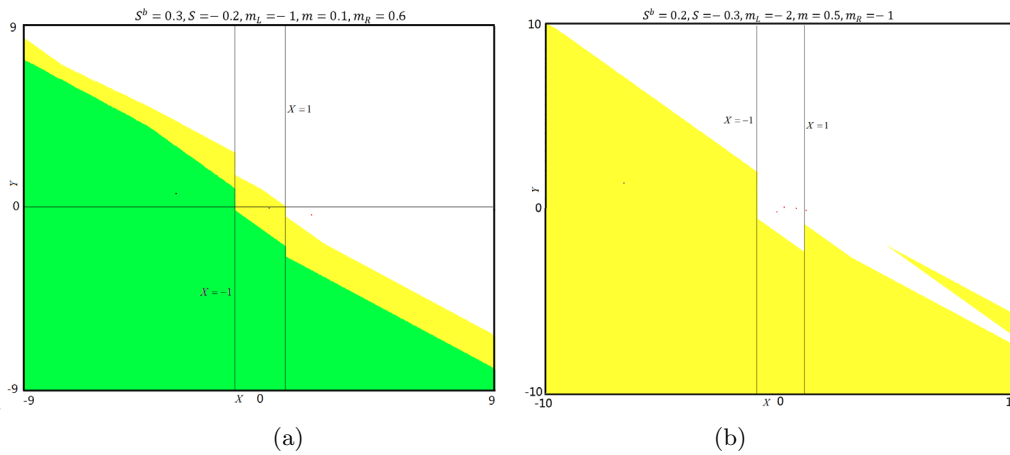


Figure 4 Basins of of coexistent attractors in phase space, (a) 3 types of fixed points and their basins obtained with $s^b = 0.2, s = -0.3, m_L = -1, m = 0.1, m_R = 0.6$, (b) 4 cycle and fixed point L^* and their basins obtained with $s^b = 0.2, s = -0.3, m_L = -2, m = 0.5, m_R = -1$

5.3 Spiral Attracting Fixed Points $-(1 + s^b) - 2\sqrt{s^b} < s < -(1 + s^b) + 2\sqrt{s^b}$

For $-(1 + s^b) - 2\sqrt{s^b} < s < -(1 + s^b) + 2\sqrt{s^b}$, all fixed points are spiral attractors. In Figure 5(a) obtained with $s^b = 0.8, s = -3, m = 4$, we show the regions associated with attracting periodic orbits in the parameter plane (m_L, m_R) . It should be pointed out that Figure 5(a) only provides the existence of stable periodic orbits. To know the exact periodicity regions in plane (m_L, m_R) , we must gave the BCB curves analytically. From (4.4), two BCB curves of the first complexity with symbol sequence $\mathcal{S} = LR$ (blue lines in Figure 5(b)) are

$$BCB_{LR}^L : -\frac{m_L + m_L s^b + m_L s + m_R + s^b m_R}{s(2 + 2s^b + s)} = -1$$

and

$$BCB_{RL}^R : -\frac{m_R + m_R s^b + m_R s + m_L + s^b m_L}{s(2 + 2s^b + s)} = 1.$$

The superscript of $BCB_S^I, I \in \{L, R\}$ indicates that the contact occurs on the I side of the border $x = -1$ or $x = 1$, and the subscript indicates the symbol sequence of the period \mathcal{S} . In the above two formulas, replace m_L with m to get two BCB curves of the first complexity with

symbol sequence $\mathcal{S} = MR$ (red lines in Figure 5(b)) are

$$BCB_{MR}^R : -\frac{m + ms^b + ms + m_R + s^b m_R}{s(2 + 2s^b + s)} = -1 \tag{5.1}$$

and

$$BCB_{MR}^L : -\frac{m + ms^b + ms + m_R + s^b m_R}{s(2 + 2s^b + s)} = 1. \tag{5.2}$$

From (4.4), two BCB curves of the first complexity with symbol sequence $\mathcal{S} = MR^2$ (purple lines in Figure 5(b)) are $BCB_{MR^2}^R : \frac{A_3}{D_3}m + \frac{B_3}{D_3}m_R = -1$, and $BCB_{MR^2}^L : \frac{A_3}{D_3}m + \frac{B_3}{D_3}m_R = 1$.

In the above two formulas, replace m with m_L to get two BCB curves of the first complexity with symbol sequence $\mathcal{S} = LR^2$ (green lines in Figure 5(b)) are $BCB_{LR^2}^L : \frac{A_3}{D_3}m_L + \frac{B_3}{D_3}m_R = -1$, and $BCB_{RLR}^R : \frac{A_3}{D_3}m_L + \frac{B_3}{D_3}m_R = 1$. The above BCB curve only involves periodic points of two character sequences, the following BCB curve involves three character sequences, which is different from what we have encountered before. BCB curves of the first complexity with symbol sequence $\mathcal{S} = LMR$ (cyan lines in Figure 5(b)) are

$$\begin{aligned} BCB_{LMR}^L &: \frac{C_3}{D_3}m_L + \frac{E_3}{D_3}m + \frac{F_3}{D_3}m_R = -1, \\ BCB_{MRL}^R &: \frac{F_3}{D_3}m_L + \frac{A_3}{D_3}m + \frac{E_3}{D_3}m_R = -1, \\ BCB_{MRL}^L &: \frac{F_3}{D_3}m_L + \frac{A_3}{D_3}m + \frac{E_3}{D_3}m_R = 1, \end{aligned} \tag{5.3}$$

where $D_3 = -s[3 + 3s^b + 3s + 3(s^b)^2 + 3s^b s + s^2]$, $A_3 = 1 + s^b + 2s + 2s^b s + (s^b)^2 + s^2$, $B_3 = 2 + 2s^b + s + s^b s + (s^b)^2$, $C_3 = 1 + s^b + 2s + 2s^b s + (s^b)^2$, $E_3 = 1 + s^b + s + (s^b)^2$, $F_3 = 1 + s^b + s^b s + (s^b)^2$.

Set parameters $s^b = 0.8, s = -3, m = 4$ and draw the above BCB curves in the plane (m_L, m_R) , we can determine the existence regions of periodic attractors. Figure 5(b) only shows BCB curves of 1 to 3 cycles and the existence regions of periodic attractors. In the overlapping periodicity regions in Figure 5(b), yellow one shows that three types of stable 3-cycles with symbol sequence LMR, LR^2 and MR^2 coexist with the fixed point R^* , and grey one 3-cycle with symbol sequence LMR and 2-cycle with symbol sequence MR coexist with two types of fixed points L^* and R^* . Comparing Figure 5(a) and (b), we know that the two-dimensional bifurcation diagram can only give types of cycles in the parameter (m_L, m_R) , can not give any information about the parameter range of various periodic attractors and coexisting attractors.

When the fixed point is a spiral attractor, Theorem 5.4 tells us that the system cannot have a saddle, so the system cannot have the complex dynamic behavior of homoclinic chaos, but because the system has multiple stable attractors coexisting, the basins of multiple attractors are entangled with each other and even chaotic boundaries may appear. Figure 6(a) shows the coexistence of at least 7 types of periodic attractors and their basin boundaries are very complicated. Figure 6(b) shows the coexistence of period-3 attractors with 3 types of symbol sequence LMR, LR^2 and MR^2 , and their basin boundaries are also very complicated.

Through the above analysis, we have the following theorem.

Theorem 5.5 *If $-(1 + s^b) - 2\sqrt{s^b} < s < -(1 + s^b) + 2\sqrt{s^b}$, map T in (3.1) has cycle attractors regardless of the value of parameters m_L, m, m_R and they may exist coexistence in most cases.*

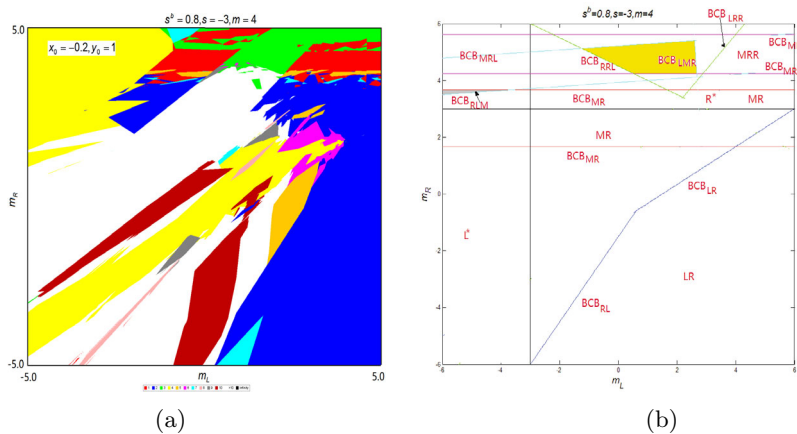


Figure 5 (a) Bifurcation diagram in plane (m_L, m_R) obtained with $s^b = 0.8, s = -3, m = 4$, (b) The existence regions of periodic attractors bounded by BCB curves obtained with $s^b = 0.8, s = -3, m = 4$

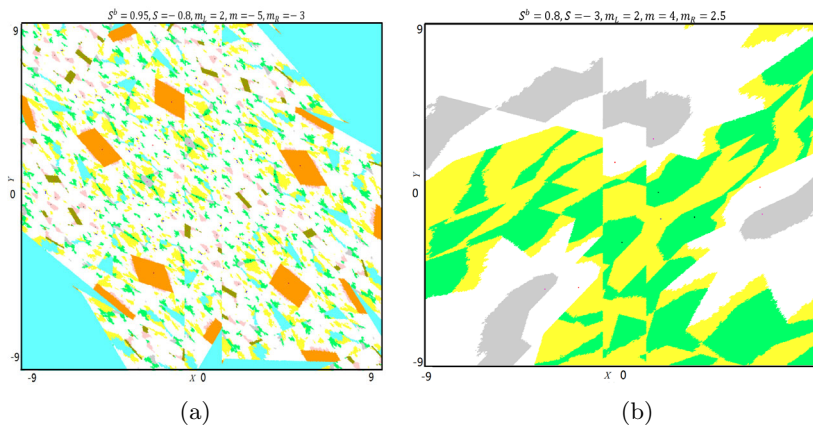


Figure 6 Basins of coexistent attractors in phase space, (a) 7 types of periodic attractors and their basins obtained with $s^b = 0.95, s = -0.8, m_L = 2, m = -5, m_R = -3$, (b) 4 types of periodic attractors and their basins obtained with $s^b = 0.8, s = -3, m_L = 2, m = 4, m_R = 2.5$

5.4 Flip Attracting Fixed Points $-2 - 2s^b < s < -(1 + s^b) - 2\sqrt{s^b}$

Similar to Subsection 5.3, I first determines the relevant BCB curves based on the two-dimensional bifurcation diagram in Figure 7(a) obtained with $s^b = 0.2, s = -2.2, m = 3$. We first analytically give the relevant BCB curves involving 4-cycles. If $S = LMRR$, we have the following BCB curves

$$BCB_{MRRL}^R : \frac{A_4}{D_4}m_L + \frac{B_4}{D_4}m + \frac{C_4}{D_4}m_R = -1,$$

$$BCB_{MRRL}^L : \frac{A_4}{D_4}m_L + \frac{B_4}{D_4}m + \frac{C_4}{D_4}m_R = 1,$$

$$BCB_{RLMR}^R : \frac{E_4}{D_4}m_L + \frac{F_4}{D_4}m + \frac{G_4}{D_4}m_R = 1. \tag{5.4}$$

If $S = LLMR$, we have the following BCB curves

$$\begin{aligned} BCB_{LLMR}^L &: \frac{H_4}{D_4}m_L + \frac{F_4}{D_4}m + \frac{K_4}{D_4}m_R = -1, \\ BCB_{LMRL}^L &: \frac{G_4}{D_4}m_L + \frac{E_4}{D_4}m + \frac{F_4}{D_4}m_R = -1 \\ BCB_{MRLL}^L &: \frac{P_4}{D_4}m_L + \frac{Q_4}{D_4}m + \frac{E_4}{D_4}m_R = 1, \end{aligned} \tag{5.5}$$

where $D_4 = -s[4+4s^b+6s+s^3+4(s^b)^3+6(s^b)^2s+4s^bs^2+4(s^b)^2+8s^bs+4s^2]$, $A_4 = 1+s^b+(s^b)^2+2s^bs+(s^b)^3+s^bs^2+2(s^b)^2s$, $B_4 = 1+s^b+3s+(s^b)^2+4s^bs+3s^2+(s^b)^3+s^3+3s^bs^2+3(s^b)^2s$, $C_4 = 2+2s^b+3s+2s^bs+2(s^b)^2+s^2+2(s^b)^3+s(s^b)^2$, $E_4 = 1+s^b+2s+(s^b)^2+2s^bs+s^2+(s^b)^3$, $F_4 = 1+s^b+s+(s^b)^2+(s^b)^2s+(s^b)^3$, $G_4 = 2+2s^b+3s+6s^bs+2(s^b)^2+3s^2+4s^bs^2+2(s^b)^3+s^3+5s(s^b)^2$, $H_4 = 2+2s^b+5s+2(s^b)^2+6s^bs+s^2+2(s^b)^3+3(s^b)^2s+3s^bs^2+s^3$, $K_4 = 1+s^b+(s^b)^2+2s^bs+(s^b)^3+2(s^b)^2s+s^bs^2$, $P_4 = 2+2s^b+s+(s^b)^2+2s^bs+s^2+(s^b)^3$, $Q_4 = 1+s^b+3s+(s^b)^2+4s^bs+3s^2+(s^b)^3+3(s^b)^2s+3s^bs^2+s^3$.

Set parameters $s^b = 0.2, s = -2.2, m = 3$ and draw relevant BCB curves of (5.1)–(5.5) in the plane (m_L, m_R) , we can determine the existence regions of periodic attractors. Figure 7(b) only shows BCB curves of 1 to 4 cycles and the existence regions of periodic attractors. In the overlapping periodicity regions in Figure 7(b), yellow one shows that three types of stable cycles with symbol sequence $LMR, LLMR$ and MR^2 coexist with the fixed point R^* , and grey one 4-cycle with symbol sequence $LLMR$ and 2-cycle with symbol sequence MR coexist with two types of fixed points L^* and R^* .

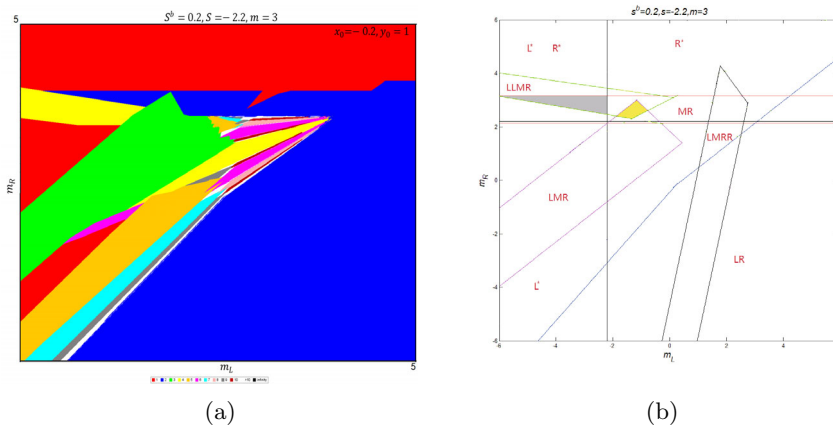


Figure 7 (a) Bifurcation diagram in plane (m_L, m_R) obtained with $s^b = 0.2, s = -2.2, m = 3$, (b) the existence regions of periodic attractors bounded by BCB curves obtained with $s^b = 0.2, s = -2.2, m = 3$

Theorem 5.6 (*Attracting fixed points and their coexistence cycles*) Suppose $-2 - 2s^b < s < -(1 + s^b) - 2\sqrt{s^b}$, consider the map T .

- 1) If $|m| < -s$, $m_L > s$, and $m_R < -s$, then trajectory from any point in the plane may converge to M^* or to coexistent attractors of a cycle and fixed point M^* ;
- 2) If $|m| < -s$, $m_L < s$, and $m_R < -s$, then attracting fixed points M^* and L^* coexist or they coexist with a cycle, and their basins are separated by preimages of the border lines $x = \pm 1$;
- 3) If $|m| < -s$, $m_L > s$, and $m_R > -s$, then attracting fixed points M^* and R^* coexist or they coexist with cycle, and their basins are separated by preimages of the border lines $x = \pm 1$;
- 4) If $m_R > m > -s$, then trajectory from any point in the plane may converge to R^* or coexistent attractors of R^* and L^* , if $m > m_R > -s$, then trajectory from any point in the plane may converge to coexistent attractors of cycles and fixed R^* (or fixed points L^* and R^*);
- 5) If $m_L < m < s$, then trajectory from any point in the plane may converge to L^* or coexistent attractors of L^* and R^* , if $m < m_L < s$, then trajectory from any point in the plane may converge to coexistent attractors of cycles and fixed L^* (or fixed points L^* and R^*).

Proof As the eigenvalues of A satisfy $-1 < \lambda_1, \lambda_2 < 0$, the eigenvalues of A^n satisfy $|\lambda_1^n| < 1, |\lambda_2^n| < 1$. Therefore, from Theorem 4.1, any periodic point can not be a saddle in this case, the boundaries of basins of coexistence attractors are thus separated by preimages of the border lines $x = \pm 1$. As the cases 3) and 5) are the symmetry of 2) and 4), we only gave the proof of the cases 1), 2) and 4), the conclusions of the cases 3) and 5) hold by Theorem 3.2.

1) As $-2 - 2s^b < s < -(1 + s^b) - 2\sqrt{s^b}$, if $|m| < -s$, $m_L > s$, and $m_R < -s$, fixed point M^* is a real flip attractor, fixed points \bar{L}^* and \bar{R}^* are virtual flip attractors. If $s < m_L < m < m_R < -s$, \bar{L}^* and \bar{R}^* locate in the middle region, trajectories from all the points in the left and right region are attracted to the middle region and then converge to M^* . If $m_L > -s$ and large enough, $m_R < s$ and small enough, then \bar{L}^* locates in the right region and \bar{R}^* in the left region, trajectories from the points in the left region may be attracted to the right region, when they pass through the middle region, some may converge to fixed point M^* , some may reach the right region and then they may be attracted back to the left region by \bar{R}^* . This will form a cycle involving only the symbols L and R . Therefore, trajectory from any point of in the plane converges to coexistent attractors of a cycle and fixed point M^* .

2) If $|m| < -s$, $m_L < s$, and $m_R < -s$, fixed points M^* and L^* are real flip attractors, fixed point \bar{R}^* is a virtual flip attractor. If $s < m_R < m < -s$, \bar{R}^* locates in the middle region and left side of M^* , then there may be cycles involving only two symbols M and R . Trajectory from any point in the right region is attracted to the middle region and left side of M^* and then is attracted back to M^* , This forms a cycle between \bar{R}^* and M^* . If $m_R < s$, \bar{R}^* locates in the left region, then there may also be cycles involving two symbols M and R . Trajectory from any point in the right region is attracted to the left region, but it must pass through the middle region, when it reaches the middle region and in the left side of M^* , it may be attracted back by M^* and form a cycle between $x = -1$ and M^* or it may pass through the border $x = -1$ and then converges to L^* . All cycles coexist with two fixed points M^* and L^* .

4) If $m_R > m > -s$, fixed point \bar{M}^* is a virtual flip attractor located in the right region,

fixed point R^* is a real flip attractor and located in the right of \overline{M}^* . Trajectory from any point in the middle region is flipped to the right region by \overline{M}^* and then it converges to R^* . If $m_L > s$, \overline{L}^* is a virtual flip attractor located in the middle or right region. Trajectory from any point in the left region is flipped to the middle region by \overline{L}^* and then to the right region by \overline{M}^* , therefore, trajectory from any point in the plane may converge to R^* . If $m_L < s$, then trajectory from any point in the left region converges to attractor L^* , and trajectory from any point in the middle and right region converges to attractor R^* . Therefore, trajectory from any point in the plane may converge to coexistent attractors of R^* and L^* . However, if $m > m_R > -s$, virtual flip attractor \overline{M}^* locates in the right region and in the right side of R^* . Some points in the middle region may be flipped to right region and in the right side of R^* , and then they may be flipped back by flip fixed point R^* , due to R^* is more closed to the middle region than \overline{M}^* . This may form a cycle between \overline{M}^* and R^* , which may coexist with R^* or with two fixed points L^* and R^* (see Figure 8).

Figure 8(a) obtained with $s^b = 0.2, s = -2.2, m_L = -1.8, m = 3, m_R = 2.3$. The parameter values are in the yellow region in Figure 7(b), thus four attractors $R^*, MR, LMR, LLMR$ coexist, and their basins are represented in grey, white, green and yellow, respectively. Figure 8(b) obtained with $s^b = 0.2, s = -2.2, m_L = -3, m = 3, m_R = 2.5$. The parameter values are in the grey region in Figure 7(b), thus four attractors $L^*, R^*, MR, LLMR$ coexist, and their basins are represented in yellow, grey, green and white, respectively.

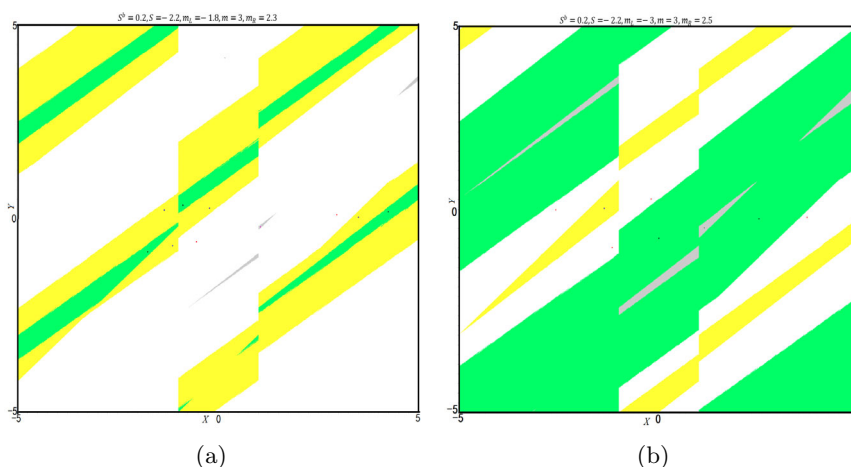


Figure 8 Basins of 4 types of coexistent attractors in phase space, (a) obtained with $s^b = 0.2, s = -2.2, m_L = -1.8, m = 3, m_R = 2.3$, (b) obtained with $s^b = 0.2, s = -2.2, m_L = -3, m = 3, m_R = 2.5$

5.5 Flip Saddle Fixed Points $s < -2 - 2s^b$

As $s < -2 - 2s^b$, all fixed points are flip saddle whether they exist or not (real or virtual). In this case, the eigenvalues of A satisfy $\lambda_1 < -1 < \lambda_2 < 0$. Dynamic behavior of the system (3.1) can be seen through the 2-dimensional bifurcation diagram of Figure 9(a) obtained with $s^b = 0.2, s = -2.5, m = 0.5$ and Figure 9(b) obtained with $s^b = 0.8, s = -3.61, m = 2$. Figure 9 shows the system (3.1) either is divergent or tends to a periodic attractor with a period

exceeding 10. From Theorem 4.1 we know that the system (3.1) has no periodic attractor, all bounded attractors are chaos or quasi-period.

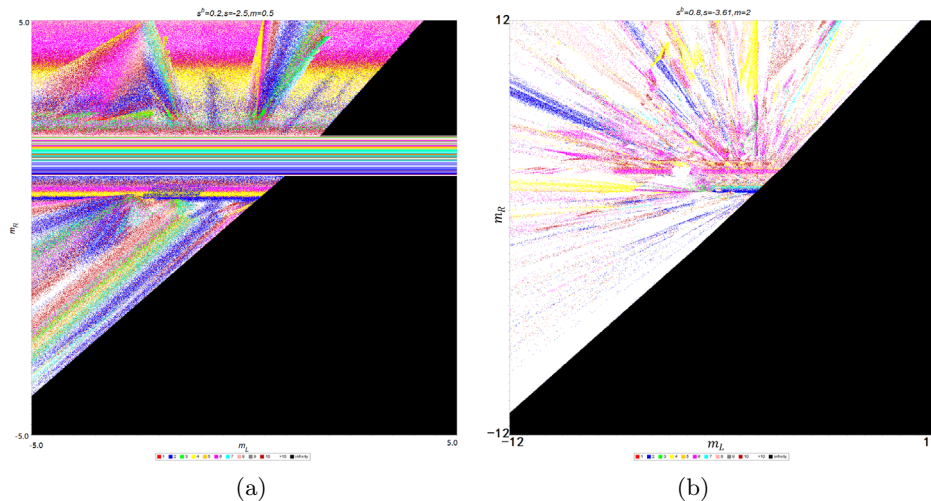


Figure 9 Bifurcation diagrams in plane (m_L, m_R) , (a) obtained with $s^b = 0.2, s = -2.5, m = 0.5$, (b) obtained with $s^b = 0.8, s = -3.61, m = 2$

Theorem 5.7 (*Divergence and bounded attractors*) Suppose $s < -2 - 2s^b$, consider the map T .

- 1) If $m_L > m > m_R$, then trajectory from any point in the plane diverges;
- 2) If $m_L > m_R > m > 0$, then trajectory from any point in the plane may diverge or converge to a chaotic or quasi-periodic attractor only involving the middle and right branches;
- 3) If $m_R < m_L < m < 0$, then trajectory from any point in the plane may diverge or converge to a chaotic or quasi-periodic attractor only involving the middle and left branches;
- 4) If $\exists c > 0$ such that $m_R - m_L > c$, then trajectory from any point in the plane may converge to chaotic or quasi-periodic attractors.

Proof As the case 3) is the symmetry of 2), we only gave the proof of the cases 1), 2) and 4), the conclusion of the case 3) holds by Theorem 3.2. As the middle fixed point is a flip saddle whether it exists or not (real or virtual), all the points in the middle region are flipped out by M^* or \overline{M}^* to the right or/and left region.

1) If $m_L > m > m_R$, we consider the following 3 cases: A) $m > -s$, B) $-s > m > s$, C) $m < s$. As C) is the symmetry of A), we only gave the proof of the cases A) and B).

A) If $m_L > m > m_R > -s$, only the fixed point R^* is a real flip saddle and the fixed points \overline{L}^* and \overline{M}^* are virtual flip saddle and locate in the right region. As \overline{L}^* locates in the far right and R^* in the far left, any point in the left and middle region is flipped to infinite along the unstable manifolds of \overline{L}^* and/or \overline{M}^* , respectively. Any point in right region and in the right side of the stable manifold of R^* is flipped to infinite along the unstable manifolds of R^* . Any point in right region and in the left side of the stable manifold of R^* is flipped to the middle and left region by R^* and then tends to infinite along the unstable manifolds of \overline{M}^* and/or \overline{L}^* .

If $m_L > m > -s > m_R$, all fixed points are virtual flip saddles and the fixed points \bar{L}^* and \bar{M}^* still locate in the right region. Any point in left and middle region is flipped to infinite along the unstable manifolds of \bar{L}^* and/or \bar{M}^* , respectively. Any point in right region is flipped to infinite along the unstable manifolds of \bar{R}^* .

B) If $-s > m > s$ and $m_L > m > m_R$, we have the 4 cases: $m_L > -s > m > s > m_R$, $-s > m_L > m > s > m_R$, $m_L > -s > m > m_R > s$ and $-s > m_L > m > m_R > s$. In all cases only the fixed point M^* is a real flip saddle and the fixed points \bar{L}^* and \bar{R}^* are virtual flip saddle. Any point in the middle region and in the right side of the stable manifold of M^* is flipped out to the right region. Symmetrically, any point in the middle region and in the left side of the stable manifold of M^* is flipped out to the left region. As R^* is in the far left and \bar{L}^* in the far right, all the points in the middle region are flipped out by M^* to the right or left region and then tend to infinite along the unstable manifolds of \bar{R}^* and/or \bar{L}^* , respectively.

2) If $m_L > m_R > -s > m > 0$, only \bar{L}^* is a virtual flip saddle and locates in the far right and M^* in the far left. Any point in middle region and in the left side of stable manifolds of M^* is flipped to the left region and then tends to infinite along the unstable manifolds of \bar{L}^* . Any point in middle region and in the right side of stable manifolds of M^* is flipped to the right region along the unstable manifolds of M^* . If R^* is not too close or too far away from M^* , that is, $\exists c_2 > c_1 > 0$, such that $0 < c_1 < m_R - m < c_2$, there is a chaotic or quasi-periodic attractor in the middle and right regions which only involves the right discontinuous border $x = 1$ (see Figure 10(a)). If $m_R - m < c_1$ or $m_R - m > c_2$, as $m_L > m_R$, trajectory from any point in the left region is flipped to infinite along the unstable manifolds of \bar{L}^* . Any point in the right region may be finally flipped to infinite along the unstable manifolds of R^* and/or \bar{L}^* . If $m_L > m_R > m > -s$, only R^* is a real flip saddle, \bar{L}^* and \bar{M}^* are virtual flip saddles locate in the far right and in the far left, respectively. Similarly, if R^* is not too close or too far away from \bar{M}^* , there is a chaotic or quasi-periodic attractor between two stable manifolds of flip saddles \bar{M}^* and R^* . If $m_L > -s > m_R > m > 0$ and $-s > m_L > m_R > m > 0$, only M^* is a real flip saddle. The point in the middle region and in the left side of M^* is flipped out to the left region then it tends to infinite along the unstable manifolds of \bar{L}^* . Some points in the middle region and in the right side of M^* are flipped out to the right region, then they may be flipped to infinite along the unstable manifolds of \bar{R}^* . If \bar{R}^* is in appropriate location, some points in the middle region and in the right side of M^* are flipped to the left side of the stable manifolds of \bar{R}^* and then is flipped back to the right side of M^* in the middle region. This may form a bounded a chaotic or quasi-periodic attractor in the middle region.

4) If $\exists c > 0$ such that $m_R - m_L > c$, trajectory from any point in the right side of the stable manifold of L^* or \bar{L}^* is finally flipped to the right region (may through the middle branch) along the unstable manifold of L^* or \bar{L}^* . But it is still in the left side of stable manifold of R^* or \bar{R}^* , it is finally flipped back to the left region (may through the middle branch) along the unstable manifold of R^* or \bar{R}^* . This may form bounded attractors which may be coexistent chaotic or quasi-periodic attractors (see Figure 10(b)). ■

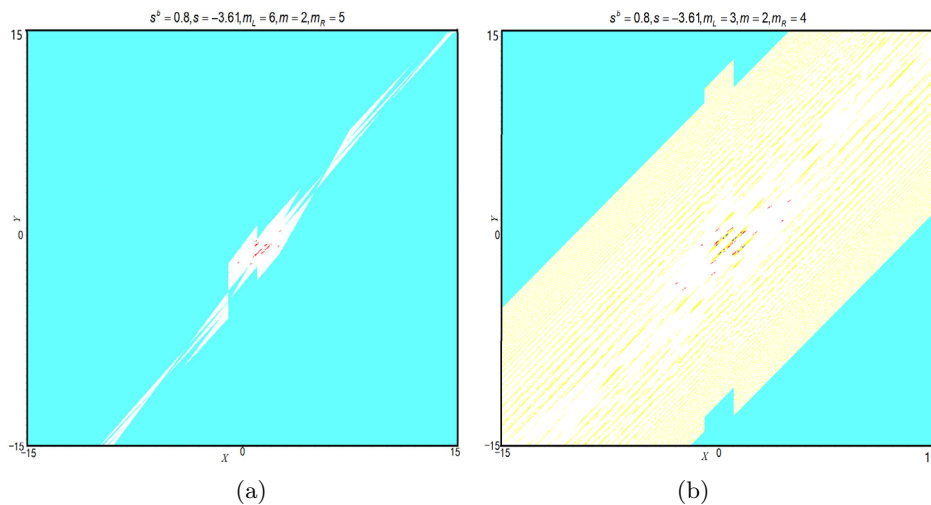


Figure 10 Basins of attractors in phase space, (a) basin of chaotic or quasi-periodic attractor obtained with $s^b = 0.8, s = -3.61, m_L = 6, m = 2, m_R = 5$, (b) basins of coexistent chaotic or quasi-periodic attractors obtained with $s^b = 0.8, s = -3.61, m_L = 3, m = 2, m_R = 4$

6 Discussions

Although there have been many models involving the interaction of different rational traders who rely on simple trading rules to produce complex internal price changes, they rarely consider the trend followers. This may be because it will lead to the establishment of a two-dimensional discontinuous model, and the research on the two-dimensional discontinuous map has not been well developed. The model we built in this article is a $2D$ PWLD map with two discontinuities. To my knowledge, there is no relevant research on this type of model. We thus hope that our analysis is also useful for the investigation of similar dynamical systems. We find that complex attractor such as chaos or quasi-period can occur only if $s > 0$ or $s < -2 - 2s^b$ and divergence often occurs in these cases. As $s > 0$ means that type 1 chartists are more aggressive than type 1 fundamentalists in bear and bull markets, respectively, and $s < -2 - 2s^b$ means that type 1 fundamentalists are much more aggressive than type 1 chartists in bear and bull markets, respectively. If $-2 - 2s^b < s < 0$, map T has no saddle periodic point and thus no chaotic attractor, but markets at least do not explode. As $m_L - m_R = m^4/z - m^3/z = [f^{2,a} + f^{2,b} - (c^{2,a} + c^{2,b})]/z$, $m_R > m_L$ means that type 2 chartists are more aggressive than type 2 fundamentalists, and vice versa. If $s > 0$ and $m_R > m_L$ or $s < -2 - 2s^b$ and $m_R < m_L$ the system (2.9) must diverge. This implies that if two types of chartists dominate two types of fundamentalists or two types of fundamentalists dominate two types of chartists, the system (2.9) must diverge. Chaos or quasi-period in the system (2.9) only occurs in the case that type 1 and type 2 chartists and fundamentalists have complementary advantages in financial markets, that is, type 1 chartists dominate fundamentalists and type 2 fundamentalists dominate chartists. That is, if two types of chartists or fundamentalists dominate financial markets at the same time, the superimposed effects are bound to cause financial markets to

collapse. Naturally, one important goal of a central authority would be to prevent the price trajectory from settling on an explosive course.

Multi-stability prevails and the basins of multi-attractors may be very complicated and even have chaotic boundary especially for the case $-(1+s^b) - 2\sqrt{s^b} < s < -2 - 2s^b$, that is, all fixed points are spiral or flip attractors. There is still the unpredictability of the financial market in these cases. It should be noted that the system (2.9) may have complicated dynamic as s^b is close to 1 (i.e., the system is adjacent to a central bifurcation occurring at $s^b = 1$). Figure 11 obtained with $m_L = 2, m = -0.2, m_R = 3$. It is 2 dimensional bifurcation diagram which is to show the possible attractors in parameter plane (s^b, s) . Figure 11(b) is a partial enlargement of Figure 11(a). Referring to Figure 1, we know that when s^b is sufficiently close to 1 (e.g., $s^b > 0.9$), the fixed point is either a saddle point (regular/flip) or a spiral attractor. From the results of Section 5, we know that if the fixed point is a saddle, the system may be divergent or converge to chaos or quasi-period. If the fixed point is a spiral attractor, although the system can not be divergent or converge to chaos or quasi-period, but multiple periodic attractors are universal with their basins very complex (see Figure 6).

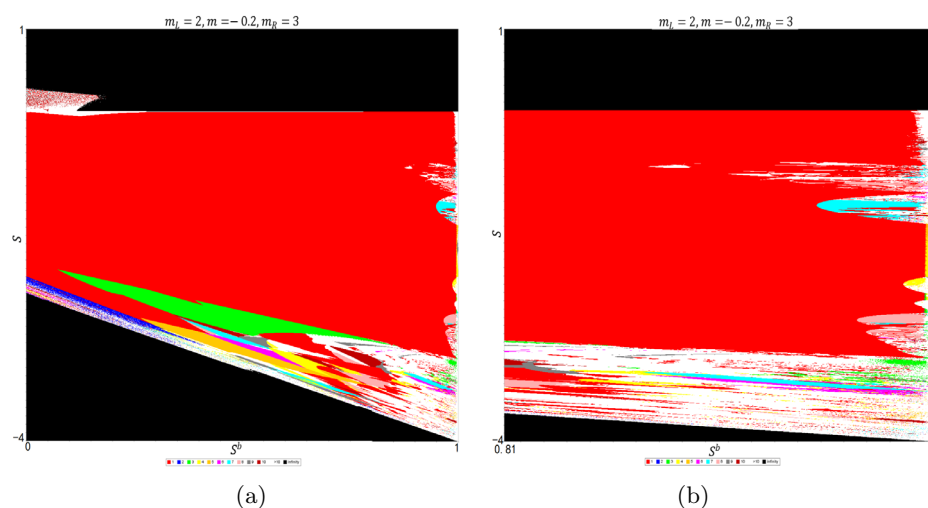


Figure 11 Bifurcation diagrams in plane (s^b, s) obtained with $m_L = 2, m = -0.2, m_R = 3$, (b) is a partial enlargement of enlargement of (a)

7 Conclusions

From the perspective of dynamics, when the fixed point is an attractor ($-2 - 2s^b < s < 0$), especially when s^b is sufficiently close to 1, it is impossible for the system to produce chaos or quasi-periodic, but it is possible to produce complex boundary of attraction domain with multiple attractors co-existing. When the fixed point is a saddle ($s > 0$ or $s < -2 - 2s^b$), the system may be chaotic or quasi-periodic ($s > 0, m_L > m_R$ or $s < -2 - 2s^b, m_L < m_R$), or divergent ($s > 0, m_L < m_R$ or $s < -2 - 2s^b, m_L > m_R$).

From an economic point of view, our simple model can help us to explain the emergence of bubbles and crashes and excessive volatility and unpredictability. If the state of our system is

unstable we think that stock market crash occurs. If the state of our system is quasi-periodic or chaotic we think that stock market is in excessive volatility and unpredictability. If our system has multiple attractors and their basins interlace or attractors sufficiently close to their basin boundary, we think that stock market is in unpredictability. Market bubbles and crash can be caused by either type 1 and type 2 chartists dominate fundamentalists or type 1 and type 2 fundamentalists (strongly) dominate chartists. Excessive volatility can be caused by type 1 and type 2 chartists and fundamentalists have complementary advantages in financial markets. Unpredictability can be caused by type 1 fundamentalists moderately dominate type 1 chartists (that is, $-2 - 2s^b < s < 0$) and higher intensity response of trend followers. At this case, the financial system is very susceptible to interference from external random factors to change its steady state, which makes the financial system extremely difficult to predict and supervise. Keeping financial markets stable requires regulators to limit excessive speculation by chartists or fundamentalists and preventing financial markets from excessive volatility requires regulators limit intensity response of trend followers to price fluctuations. Our main results may be summarized as follows:

- Synergistic dominance among type 1 and type 2 traders leads to bubbles and and crashes in financial markets.
- Complementary dominance among type 1 and type 2 traders leads to excessive volatility in financial markets.
- Type 1 fundamentalists moderately dominate type 1 chartists and high intensity response of trend followers to price fluctuations may lead to unpredictability in financial markets.

Conflict of Interest

The authors declare no conflict of interest.

References

- [1] Hommes A C, Evolutionary selection of individual expectations and aggregate outcomes in asset pricing experiments, *American Econ. J.: Microeconomics*, 2012, **4**(4): 35–64.
- [2] Brock W and Hommes C, Heterogeneous beliefs and routes to chaos in a simple asset pricing model, *J. of Econ. Dyn. and Control*, 1998, **22**: 1235–1274.
- [3] Chiarella C, Dieci R, and He X Z, Heterogeneity, market mechanisms, and asset price dynamics, Eds. by Hens T and Schenk-Hopp K R, *Handbook of Financial Markets: Dynamics and Evolution*, North-Holland, Amsterdam, 2009.
- [4] Hommes C, *Behavioral Rationality and Heterogeneous Expectations in Complex Economic Systems*, Cambridge University Press, Cambridge, U.K., 2013.
- [5] Tramontana F, Gardini L, and Puu T, Duopoly games with alternative technologies, *J. Econ. Dyn. Control*, 2009, **33**: 250–265.

-
- [6] Westerhoff F, Exchange rate dynamics: A nonlinear survey, Ed. by Rosser J B, *Handbook of Research on Complexity*, Cheltenham, Edward Elgar, 2009.
- [7] Brock W A, Hommes C H, and Wagener F, More hedging instruments may destabilize markets, *J. of Econ. Dyn. Control*, 2009, **33**(11): 1912–1928.
- [8] Lux T, Stochastic Behavioural Asset-Pricing Models And The Stylized Facts, Eds. by Hens T, Schenk-Hopp K R, *Handbook of Financial Markets: Dynamics and Evolution*, North Holland, Amsterdam, 2009, 161–216.
- [9] LeBaron B, Agent-based computational finance, Eds. by Tesfatsion L and Judd K, *Handbook of Computational Economics, Agent-Based Computational Economics*, North Holland, 2006, **2**: 1187–1233.
- [10] Naimzada A K and Ricchiuti G, Heterogeneous fundamentalists and imitative processes, *Appl. Math Comput.*, 2008, **199**(1): 171–80.
- [11] Naimzada A K and Ricchiuti G, Dynamic effects of increasing heterogeneity in financial markets, *Chaos Solitons & Fractal*, 2009, **41**(4): 1764–72.
- [12] Westerhoff F, Multiasset market dynamics, *Macroecon. Dyn.*, 2004, **8**(5): 96–616.
- [13] Agliari A, Naimzada A, and Pecora N, Boom-bust dynamics in a stock market participation model with heterogeneous traders, *J Econ. Dyn. Control*, 2018, **91**: 458–68.
- [14] Hommes C and LeBaron B, *Computational Economics: Heterogeneous Agent Modeling*, Elsevier, 2018.
- [15] Polach J and Kukacka J, Prospect theory in the heterogeneous agent model, *J. Econ. Interact. Coordin.*, 2019, **14**(1): 147–174.
- [16] Ellen S T and Verschoor W, Heterogeneous beliefs and asset price dynamics: A survey of recent evidence, *Uncertainty, Expectations and Asset Price Dynamics*, Springer, 2018, 53–79.
- [17] Jahanshahi H, Sajjadi S S, Bekiros S, et al., On the development of variable-order fractional hyperchaotic economic system with a nonlinear model predictive controller, *Chaos Solitons & Fractals*, 2021, **144**: 110698.
- [18] Jahanshahi H, Yousefpour A, Wei Z, et al., A financial hyperchaotic system with coexisting attractors: Dynamic investigation, entropy analysis, control and synchronization, *Chaos, Solitons & Fractals*, 2019, **126**: 66–77.
- [19] Ay A, Hj B, Mp C, et al., A fractional-order hyper-chaotic economic system with transient chaos, *Chaos, Solitons & Fractals*, 2020, **130**(C): 109400–109400.
- [20] Day R and Huang W, Bulls, bears and market sheep, *J. Econ. Behav. Org.*, 1990, **14**: 299–329.
- [21] Day R, Complex dynamics, market mediation and stock price behavior, *North American Actuarial J.*, 1997, **1**: 6–21.
- [22] DeGrauwe P, Dewachter H, and Embrechts M, *Exchange Rate Theories, Chaotic Models of the Foreign Exchange Market*, Oxford, Blackwell, 1993.
- [23] Farmer J D and Joshi S, The price dynamics of common trading strategies, *J. of Econ. Behavior and Org.*, 2002, **49**: 149–171.
- [24] Tramontana F, Westerhoff F, and Gardini L, On the complicated price dynamics of a simple one-dimensional discontinuous financial market model with heterogeneous interacting traders, *J. of Econ. Beha. and Org.*, 2010, **74**: 187–205.
- [25] Tramontana F, Westerhoff F, and Gardini L, The bull and bear market model of Huang and Day: Some extensions and new results, *J. of Econ. Dyn. and Control*, 2013, **37**: 2351–2370.
- [26] Tramontana F, Westerhoff F, and Gardini L, One-dimensional maps with two discontinuity points

- and three linear branches: Mathematical lessons for understanding the dynamics of financial markets, *Decisions in Econ. and Finance*, 2014, **37**: 27–51.
- [27] Tramontana F, Westerhoff F, and Gardini L, A simple financial market model with chartists and fundamentalists: Market entry levels and discontinuities, *Math. and Comp. in Simu.*, 2015, **108**: 16–40.
- [28] Lux T, Herd behavior, bubbles and crashes, *Econ. J.*, 1995, **105**: 881–896.
- [29] Gardini L, Merlone U, and Tramontana F, Inertia in binary choices: Continuity breaking and big-bang bifurcation points, *J. of Econ. Behavior and Org.*, 2011, **80**: 153–167.
- [30] Puu T, The Hicksian trade cycle with floor and ceiling dependent on capital stock, *J. Econ. Dyn. Control*, 2007, **31**: 575–592.
- [31] Gardini L, Avrutin V, and Sushko I, Codimension-2 border collision bifurcations in one-dimensional discontinuous piecewise smooth maps, *Int. J. Bifur. Chaos*, 2014, **24**: 1450024–1–30
- [32] Gardini L and Tramontana F, Border collision bifurcation curves and their classification in a family of 1D discontinuous maps, *Chaos, Solitons & Fractals*, 2011, **44**(4–5): 248–259.
- [33] Gardini L and Tramontana F, Border-collision bifurcations in 1D piecewise-linear maps and Leonovs approach, *Int. J. of Bifur. and Chaos*, 2010, **20**(10): 3085–3104.
- [34] Gardini L and Tramontana F, Border collision bifurcations in 1D PWL map with one discontinuity use of the first return map, *Int. J. of Bifur. and Chaos*, 2010, **20**(11): 3259–3574.
- [35] Sushko I, Gardini L, and Avrutin V, Nonsmooth one-dimensional maps: Some basic concepts and definitions, *J. of Dif. Equ. and Appl.*, 2016, **22**(12): 1816–1870.
- [36] Bischi G and Merlone U, Global dynamics in binary choice models with social influence, *The J. of Math. Sociology*, 2009, **33**: 277–302.
- [37] Bischi G, Gardini L, and Tramontana F, Bifurcation curves in discontinuous maps, *Discrete and Continuous Dyn. Systems-Series B*, 2012, **13**(2): 249–267.
- [38] Gu E G, On the price dynamics of a two dimensional financial market model with entry levels, *Complexity*, 2020, Article ID: 3654083, 23 Pages.
- [39] Gu E G and Guo J, BCB curves and contact bifurcations in piecewise linear discontinuous map arising in a financial market, *Int. J. of Bifur. and Chaos*, 2019, **29**(2): 195002–195035.
- [40] Banerjee S, Ranjan P, and Grebogi C, Bifurcations in two dimensional piecewise smooth maps-theory and applications in switching circuits, *IEEE Trans. Circuits. Syst. I*, 2000, **47**(5): 633–643.
- [41] Chiarella C, Dieci R, and Gardini L, The dynamic interaction of speculation and diversification, *Appl Math Finance*, 2005, **12**(1): 17–52.